iomac
International Operational Modal Analysis Conference

11th International Operational Modal Analysis Conference

20 - 23 May 2025 | Rennes, France

A novel lagged estimation framework for sparsely observed systems supplemented with virtual measurements sampled in delayed time

Shereena OA[1], *Subhamoy Sen*[1], *and Laurent Mevel*[2]

[1] i4S Laboratory, Indian Institute of Technology Mandi, Mandi, HP, India, subhamoy@iitmandi.ac.in

[2] Univ. Gustave Eiffel, Inria, COSYS-SII, I4S Team, France, laurent.Mevel@inria.fr

ABSTRACT

This study introduces an innovative framework for reconstructing structural responses using an enhanced measurement vector augmented with time-lagged measurements, as if obtained from virtual sensors, to tackle issues related to sparse instrumentation and complex system dimensions. By including delayed embeddings in the measurement vectors, this method greatly improves the observability of structural states, ensuring precise state estimation even when systems are sparsely monitored. The embedding approach adeptly counters the limitations posed by physical instrumentation, facilitating reliable monitoring even in demanding situations.

To further enhance the computational efficiency, the system dynamics are characterized in the modal domain, where mode shapes and natural frequencies are modulated with location-specific health variables. These variables facilitate the construction of a simplified state-space model, which is subsequently integrated into a Bayesian filtering-based estimation framework. By conducting filtering operations in modal coordinates, this strategy achieves notable computational efficiency without sacrificing precision. The framework undergoes testing on simplified linear time-invariant (LTI) systems utilizing the Kalman filter in the modal domain, with observability analysis informing sensor allocation. The findings demonstrate that utilizing time-lagged embedding along with reduced-order modeling within the modal domain can enhance the accuracy of state estimation, all while reducing the requirement for extensive instrumentation. The method's flexibility to adapt to more complex, time-variant systems emphasizes its promise for advanced structural health monitoring and parameter estimation.

Keywords: Virtual Sensor, Mode shape reconstruction, Condition monitoring, State estimation, Limited data, High dimensionality, Large structures.

1. INTRODUCTION

Data loss is inevitable in real-world applications and can occur due to various factors [1]. Ensuring sufficient sensor data availability, particularly at critical locations, is essential for the effective performance of structural health monitoring (SHM) systems [2]. However, for large structures or those with high-degree-of-freedom finite element models, instrumentation and computational modeling become increasingly challenging due to cost constraints, accessibility issues, and computational burden [3, 4]. Additionally, limited data availability, whether due to unexpected sensor failures or economic constraints, combined with high-dimensional computational models, poses significant challenges for traditional vibration-based health assessment methods. These issues often lead to observability limitations and solution non-uniqueness, which are typical characteristics of ill-posed systems, ultimately resulting in inaccurate response predictions at unobserved locations. Conversely, accurate response reconstruction is critical to maintaining the effectiveness of health monitoring processes and ensuring reliable damage detection and system assessment.

Further, model-free approaches, though promising, require large volumes of data, and are not robust in locating and quantifying damage. This necessitates the need for model-dependent approaches, such as Bayesian filters. Bayesian filtering frameworks, encompassing methods such as the Extended Kalman Filter (EKF), Ensemble Kalman Filter (EnKF), Unscented Kalman Filter (UKF), and Particle Filter (PF), offer powerful tools for system health estimation. Unlike the modal-domain, and data-driven approaches, real time monitoring is feasible with Bayesian filtering approaches, which is important in detecting the chances of failures in due time, as these techniques relies on recursive estimation. Smoothing techniques, such as fixed-lag smoothing integrated into Kalman filters, estimate states with a lag by incorporating future measurements into the model (i.e. $p(x_{k-L}/y_1, y_2, ...y_k)$). However, this does not fully resolve the observability issues. To address this, the proposed technique employs a delay embedding strategy to construct an augmented measurement vector, effectively increasing its dimensionality and enhancing observability.

Response reconstructions could be performed via state estimation approaches. The estimation process if performed within a reduced order space, evidently alleviates the high dimensionality issues. Also, the delay embedded measurement models improves the overall observability [5]. Combining the above strategies, this work proposes a novel response construction strategy, that simultaneously addresses the observability and high dimensionality challenges, within a Bayesian filtering environment.

2. METHODOLOGY

Consider an n-degree-of-freedom (*dof*) linear dynamic system obtained through spatial discretization, typically using the Finite Element Method (FEM), governed by the following equation:

$$\mathbf{M}\ddot{\mathbf{u}}(t) + \mathbf{C}\dot{\mathbf{u}}(t) + \mathbf{K}\mathbf{u}(t) = \mathbf{f}(t), \tag{1}$$

where matrix $\mathbf{M} \in \mathbb{R}^{n\times n}$, $\mathbf{C} \in \mathbb{R}^{n\times n}$ and $\mathbf{K} \in \mathbb{R}^{n\times n}$ represent mass, damping and stiffness matrices respectively. The displacement vector and its derivatives are given by $\mathbf{u}(t),\ \dot{\mathbf{u}}(t),\ \ddot{\mathbf{u}}(t) \in \mathbb{R}^n$ respectively, while the external force vector is $\mathbf{f}(t) \in \mathbb{R}^m$.

In reduced-order modelling, the displacement field is approximated by summing the responses of the dominant r modes through a truncated modal expansion:

$$\mathbf{u}(t) \approx \boldsymbol{\phi}_r \mathbf{q}_r(t), \tag{2}$$

where $\boldsymbol{\phi}_r \in \mathbb{R}^{n\times r}$ denotes reduced modal matrix containing the first r dominant modes and $\mathbf{q}_r(t) \in \mathbb{R}^r$ denotes the displacement vector in generalized modal coordinates.

Substituting this into the governing equation and pre-multiplying by $\boldsymbol{\phi}_r^T$, we obtain the reduced-order system:

$$\boldsymbol{\mathcal{M}}_r\ddot{\mathbf{q}}_r(t) + \boldsymbol{\mathcal{C}}_r\dot{\mathbf{q}}_r(t) + \boldsymbol{\mathcal{K}}_r\mathbf{q}_r(t) = \boldsymbol{\phi}_r^T\mathbf{f}(t), \tag{3}$$

where the reduced-order system matrices can be obtained as $\boldsymbol{\mathcal{M}}_r = \boldsymbol{\phi}_r^T \mathbf{M} \boldsymbol{\phi}_r$, $\boldsymbol{\mathcal{C}}_r = \boldsymbol{\phi}_r^T \mathbf{C} \boldsymbol{\phi}_r$ and $\boldsymbol{\mathcal{K}}_r = \boldsymbol{\phi}_r^T \mathbf{K} \boldsymbol{\phi}_r \in \mathbb{R}^{r \times r}$.

Further defining the state vector $\mathbf{x}_r(t) = \begin{bmatrix} \mathbf{q}_r^T(t) & \dot{\mathbf{q}}_r^T(t) \end{bmatrix}^T \in \mathbb{R}^{2r}$, the reduced-order system can be rewritten in state-space form as:

$$\dot{\mathbf{x}}_r(t) = \mathbf{A}_c \mathbf{x}_r(t) + \mathbf{B}_c \mathbf{f}(t), \tag{4}$$

with $\mathbf{A}_c = \begin{bmatrix} \mathbf{0}_{r \times r} & \mathbf{I}_{r \times r} \\ -\boldsymbol{\mathcal{M}}_r^{-1} \boldsymbol{\mathcal{K}}_r & -\boldsymbol{\mathcal{M}}_r^{-1} \boldsymbol{\mathcal{C}}_r \end{bmatrix}_{r \times r}$ and $\mathbf{B_c} = \begin{bmatrix} \mathbf{0}_{r \times r} \\ \boldsymbol{\mathcal{M}}_r^{-1} \boldsymbol{\phi}_r^T \end{bmatrix}_{r \times m}$ are the state and input matrices, respectively. Eventually, the system's order is substantially reduced from $2n$ (full-state) to $2r$ (reduced modal domain) by utilizing the reduced state vector $\mathbf{x}_r(t) \in \mathbb{R}^{2r}$. The unobserved reduced order states are further observed as accelerations through the following measurement model wherein only a subset of accelerations are observed selected with the help of a Boolean selection matrix $\mathbf{S}_{p \times n}$,

$$\mathbf{y}(t) = \mathbf{S} \left[\mathbf{C}_c \mathbf{x}_r(t) + \mathbf{D}_c \mathbf{f}(t) \right] + \mathbf{v}(t), \tag{5}$$

with $\mathbf{C}_c = \boldsymbol{\phi}_r \begin{bmatrix} -\boldsymbol{\mathcal{M}}_r^{-1} \mathbf{K}_r & -\boldsymbol{\mathcal{M}}_r^{-1} \mathbf{C}_r \end{bmatrix}$ and $\mathbf{D}_c = \boldsymbol{\phi}_r \boldsymbol{\mathcal{M}}_r^{-1} \boldsymbol{\phi}_r^T$.

Since the sampled responses from the structure are obtained as discrete-time signals, the continuous model needs to be reformulated into a discrete-time state-space representation, as shown below:

$$\begin{array}{lll} \text{Process equation:} & \mathbf{x}_k & = \mathbf{A}\mathbf{x}_{k-1} + \mathbf{B}\boldsymbol{\gamma}_k + \mathbf{w}_k \\ \text{Measurement equation:} & \mathbf{y}_k & = \mathbf{C}\mathbf{x}_k + \mathbf{D}\boldsymbol{\gamma}_k + \mathbf{v}_k \end{array} \tag{6}$$

with $\mathbf{x}_k \in \mathbb{R}^{2n}$, $\mathbf{y}_k \in \mathbb{R}^m$, and the unmeasured ambient noise $\boldsymbol{\gamma}_k \in \mathbb{R}^s$ denoting state, output, and input in discrete time. The matrices $\mathbf{A}$, $\mathbf{B}$, $\mathbf{C}$, and $\mathbf{D}$ represent the discrete-time state transition, input, measurement, and direct transition matrices, respectively. For a detailed formulation of these system matrices, readers are referred to the work of [6]. The pertinent discrete representations of the noise processes are $\mathbf{w}_k$ and $\mathbf{v}_k$, corresponding to their continuous entities, respectively, and are characterized using SWGN models with covariances $\mathbf{Q}$ and $\mathbf{R}$.

2.1. Temporal virtual sensor-based formulations within Kalman filter

This research further employs delay embedding in the measurement model to tackle the key issue of limited data emphasized in this study. Observability of the entire system appears to diminish with inferior sensor setups and/or fewer measurements in $\mathbf{y}_k$. Despite the constraints of the sensor configuration, this work investigates the potential to boost observability and reconstruction precision through temporal augmentation of the measurement vector. The model with temporal virtual measurements is extended by z virtual layers. The choice for z relies on the assumption that the improved observation vector dimension $(z+1)p > 2n+1$, as supported by Taken's theorem [7].

With the augmented measurement vector $\bar{\mathbf{y}}_k \in \mathbb{R}^{zp}$ defined as

$$\bar{\mathbf{y}}_k = \begin{bmatrix} \mathbf{y}_k^T & \mathbf{y}_{k+1}^T & \cdots & \mathbf{y}_{k+z}^T \end{bmatrix}^T, \tag{7}$$

the mapping of the current state to both present and future measurements is reformulated, leading to a redefined measurement model. This formulation is systematically outlined below.

To establish the relationship between the current state $\mathbf{x}_k$ and the future measurement $\mathbf{y}_{k+1}$, we define the measurement model at the $(k+1)^{th}$ time instant as

$$\mathbf{y}_{k+1} = \mathbf{C}\mathbf{x}_{k+1} + \mathbf{D}\boldsymbol{\gamma}_{k+1} + \mathbf{v}_{k+1}. \tag{8}$$

By expressing $\mathbf{x}_{k+1}$ in terms of $\mathbf{x}_k$, the equation can be expanded as

$$\mathbf{y}_{k+1} = [\mathbf{CA}]\mathbf{x}_k + [\mathbf{CB} + \mathbf{D}]\boldsymbol{\gamma}_{k+1} + \mathbf{C}\mathbf{w}_{k+1} + \mathbf{v}_{k+1}. \tag{9}$$

A similar approach can be utilized to establish the relationship between $\mathbf{x}_k$ and the measurement at the $(k+i)^{th}$ time instant, $\mathbf{y}_{k+i}$ for $i = 1, \cdots, z$. By aggregating responses up to $\mathbf{y}_{k+z}$ for $\mathbf{x}_k$, additional z layers are eventually incorporated into the measurement vector. For brevity, the augmented measurement model for the specific case of $z = 2$ is formulated as ,

$$\bar{\mathbf{y}}_k = \begin{bmatrix} \boldsymbol{\mathcal{C}} & \vdots & \boldsymbol{\mathcal{D}} \end{bmatrix} \begin{bmatrix} \mathbf{x}_k \\ \bar{\boldsymbol{\gamma}}_k \end{bmatrix} + \boldsymbol{\mathcal{W}} \bar{\mathbf{w}}_k + \bar{\mathbf{v}}_k. \tag{10}$$

wherein, $\bar{\boldsymbol{\gamma}}_k = \{\boldsymbol{\gamma}_k^T;\ \boldsymbol{\gamma}_{k+1}^T;\ \boldsymbol{\gamma}_{k+2}^T\}^T$, $\bar{\mathbf{w}}_k = \{\mathbf{w}_k^T;\ \mathbf{w}_{k+1}^T;\ \mathbf{w}_{k+2}^T\}^T$ and $\bar{\mathbf{v}}_k = \{\mathbf{v}_k^T;\ \mathbf{v}_{k+1}^T;\ \mathbf{v}_{k+2}^T\}^T$. Accordingly, $\bar{\mathbf{w}}_k$ and $\bar{\mathbf{v}}_k$ are characterized by the covariance structures $\bar{\mathbf{Q}}_k$ and $\bar{\mathbf{R}}_k$ respectively. Additionally, $\boldsymbol{\mathcal{C}}$, $\boldsymbol{\mathcal{D}}$, and $\boldsymbol{\mathcal{W}}$ are defined as,

$$\boldsymbol{\mathcal{C}} = \begin{bmatrix} \mathbf{C} \\ \mathbf{CA} \\ \mathbf{CAA} \end{bmatrix}, \quad \boldsymbol{\mathcal{D}} = \begin{bmatrix} \mathbf{D} & \mathbf{0} & \mathbf{0} \\ \mathbf{0} & \mathbf{CB}+\mathbf{D} & \mathbf{0} \\ \mathbf{0} & \mathbf{CAB} & \mathbf{CB}+\mathbf{D} \end{bmatrix}, \quad \boldsymbol{\mathcal{W}} = \begin{bmatrix} \mathbf{0} & \mathbf{0} & \mathbf{0} \\ \mathbf{0} & \mathbf{C} & \mathbf{0} \\ \mathbf{0} & \mathbf{CA} & \mathbf{C} \end{bmatrix}. \tag{11}$$

Further, by combining Eq. (6) and Eq. (10), and subsequently reorganizing the terms, the discrete-time state-space representation is obtained as:

$$\begin{aligned} \mathbf{x}_k &= \mathbf{A}\mathbf{x}_{k-1} + \boldsymbol{\mathcal{B}}\bar{\boldsymbol{\gamma}}_k + \tilde{\mathbf{w}}_k, \\ \bar{\mathbf{y}}_k &= \boldsymbol{\mathcal{C}}\mathbf{x}_k + \boldsymbol{\mathcal{D}}\bar{\boldsymbol{\gamma}}_k + \tilde{\mathbf{v}}_k. \end{aligned} \tag{12}$$

with $\boldsymbol{\mathcal{B}} = \begin{bmatrix} \mathbf{B} & \mathbf{0} & \mathbf{0} \end{bmatrix}$, $\tilde{\mathbf{w}}_k = \begin{bmatrix} \mathbf{I} & \mathbf{0} & \mathbf{0} \end{bmatrix} \bar{\mathbf{w}}_k$ and $\tilde{\mathbf{v}}_k = \boldsymbol{\mathcal{W}}\bar{\mathbf{w}}_k + \bar{\mathbf{v}}_k$.
Here, $\tilde{\mathbf{w}}_k$ and $\tilde{\mathbf{v}}_k$ represent the process and measurement uncertainties in this extended formulation, characterized by the covariance matrices $\tilde{\mathbf{Q}}$ and $\tilde{\mathbf{R}}$, respectively. The expressions for these covariance matrices can be derived from the preceding formulation, though they are not explicitly detailed here for the sake of conciseness.

3. NUMERICAL ILLUSTRATION

The numerical validation is performed on a 12 m span beam-like structure with one end fixed, and the other simply supported. The model is discretized into twelve 3D beam elements, each defined by two boundary nodes with six degrees of freedom (*dof*s) in each node, resulting in a total of 58 free *dof*s. The geometrical and material properties of the structure are provided in Table 1.

Table 1: Properties of the numerical beam model

Width	Depth	Area	E	G	I_x	I_y	J	ρ
2.5	0.5	1.25	3.60×10^{10}	1.64×10^{10}	2.6×10^{-2}	0.65	0.68	2400

The symbols carry the usual meanings. All the quantities are expressed in their respective SI units.

An ambient vibration, modeled as a zero-mean stationary white Gaussian noise (SWGN) process with unit covariance, is assumed to act across all degrees of freedom (*DOFs*). Additionally, arbitrary instantaneous triangular pulses, simulating vehicular loads, are applied exclusively to the vertical *DOFs*. Consequently, the vertical *DOFs* experience intermittent and randomly occurring impact forces, characterized by a stochastic magnitude following a normal distribution $N(1, 10^4)$. To replicate realistic field conditions, the measurement data are intentionally corrupted with 0.1-5% noise (*snr*).

An initial study was conducted to investigate the effects of the reduction in the order of the state model and the order of the measurement model, both individually and in relation to each other. As expected,

when all modes were included in the state model and all 58 *DOFs* (rotational and translational in all three directions) were instrumented, the estimates closely matched the original time series. For brevity, only the modal displacement response corresponding to the first dominant mode is presented (*see* Figure 1a).

In contrast, when the number of sensors was reduced to 9 (instrumenting only the vertical *DOFs*), the estimates deteriorated with the larger state model order and the lower observation model order (*see* Figure 1b). Further numerical investigations, incorporating only the first three dominant modes to reduce the state model order, yielded improved estimates comparable to the original results (cf. Figure 4). Furthermore, layering in the measurement vector further refined the estimates, enhancing their accuracy.

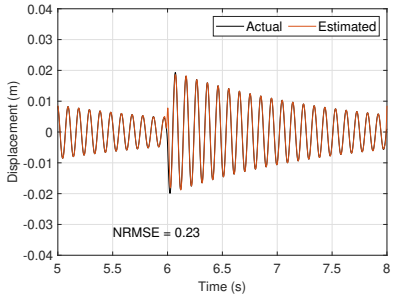

(a) 58 sensors

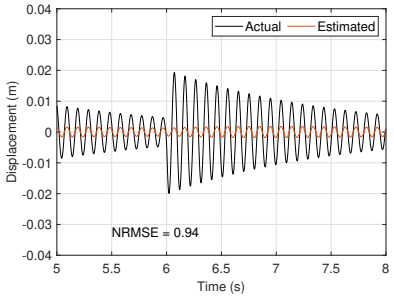

(b) 9 sensors

Figure 1: Modal response estimates corresponding to first dominant mode, considering all modes in state model

Two observation scenarios are considered. In the first scenario ($S5$), measurements are taken from a subset of five vertical *DOFs* (e.g., [8, 20, 26, 32, 44]). In the second scenario ($S9$), all vertical *DOFs* are instrumented, though this remains a relatively small subset compared to the total of 58 *DOFs*. The simulated acceleration responses under these loading conditions are sampled at 1000 **Hz** over a 20 **s** duration. These responses are then processed using frequency domain decomposition to extract the dominant frequencies: 10.3 **Hz**, 25.8 **Hz**, and 43.4 **Hz**. Only the corresponding modal components are retained for the subsequent response reconstruction process.

While the selected modes capture most of the system's output response, restricting the reconstruction to only the dominant modes may still result in some loss of modal information, although insignificant yet capable of enhancing measurement uncertainty in the estimation process. Consequently, when utilizing sampled acceleration time histories, a transformation is applied to the time-domain data by filtering out higher-order mode contributions. A band-pass filter is employed to eliminate frequency components outside the range of $[5 - 55]$ **Hz**, ensuring a reliable and accurate reconstruction assessment.

Furthermore, state estimation is conducted using the proposed Kalman filtering approach with augmented sensor data, under the assumption of known input statistics. Given that the instantaneous force impulses occur only at isolated time instances, they are disregarded in defining input force statistics to be used for estimation. In accordance with the modified state-space formulations, the Kalman gains are computed and incorporated into the estimation framework.

3.1. Response reconstruction

The primary objective of this study is to evaluate the effectiveness of delayed measurement augmentation in enhancing observability, as reflected in the estimation error. To this end, two types of responses are analyzed: those obtained at measured (observed) locations and those at unmeasured (unobserved) locations. While the estimation accuracy at measured locations demonstrates the algorithm's ability to filter out noise, the predicted response at unmeasured locations highlights its capability for accurately reconstructing unknown measurements.

A comprehensive experimental analysis is conducted, wherein the estimation error is assessed for both observed and unobserved locations as the proposed algorithm operates with an increasing number of augmented layers. Additionally, a baseline scenario without data augmentation is considered for com-

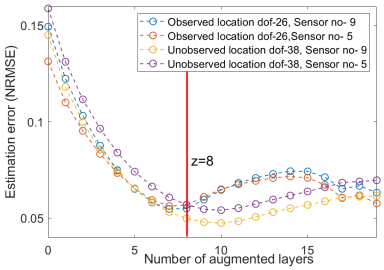

Figure 2: Estimation error decrement with measurement augmentation

parison. The estimation errors are quantified using the normalized root mean square error (NRMSE) and are presented in Figure 2. The results confirm that incorporating additional layers improves estimation accuracy for both location types up to a certain threshold. Beyond this point, however, further layering ceases to yield significant improvements. This plateau in performance is attributed to computational intractability and the diminishing observability of states due to the damping effect in highly delayed responses. Accordingly, this study identifies an optimal number of augmentation layers necessary to maximize the benefits of measurement augmentation while maintaining computational feasibility.

In line with this, the reconstructed temporal sequences obtained through the proposed estimation approach, incorporating their respective optimal layers of data augmentation, are presented in Figure 3. It has been observed that the impact of delay embedding for enhancing observability is markedly significant in improving the precision of measurement estimations (*refer to* Figure 3), which is a highly favorable outcome. The improvement in prediction accuracy strongly supports the potential extension of the model for applications in parameter estimation tasks, including those related to health metrics, which will be explored in our future studies.

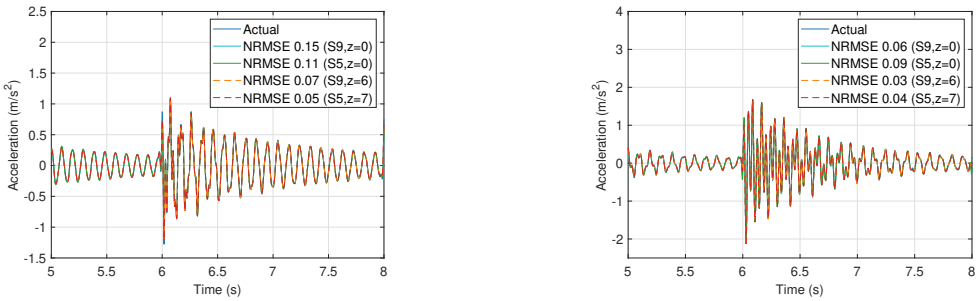

(a) at an observed location, *dof* 26 **(b)** at an unobserved location, *dof* 38

Figure 3: Estimated acceleration time histories.

3.2. Effect of Layering on State Estimates

Since the estimation is conducted within a reduced-order modal space, the modal responses corresponding to the first three dominant modes have been computed. The resulting modal displacements, obtained with different levels of layering, are presented in Figure 4. For the scenario involving nine sensors, six additional layers ($z = 6$) were incorporated, while for the scenario with five sensors, seven additional layers ($z = 7$) were used. These configurations aim to enhance the accuracy of state estimation by leveraging delayed measurement augmentation.

3.3. Effect of noise levels

Data augmentation also holds the potential to mitigate the adverse effects of noise. Since a larger dataset provides a more robust basis for inference, this study examines the performance of the proposed approach under varying levels of noise contamination. In this context, SWGN with a signal-to-noise ratio (*SNR*)

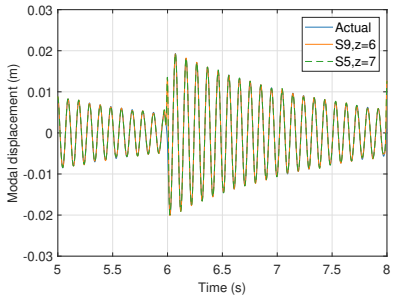

(a) Mode 1

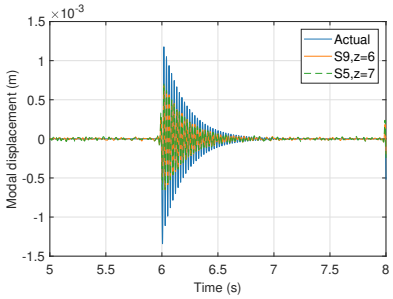

(b) Mode 3

Figure 4: Estimated modal responses corresponding to the specified dominant mode.

ranging from 0.1% to 5% has been introduced to evaluate the effectiveness of the method.

As observed in Figure 5, increasing the number of augmented layers significantly attenuates the impact of noise. This finding is particularly advantageous in scenarios where the response is highly contaminated or where the signal strength is inherently weak, leading to higher relative noise levels under a constant sensor noise condition.

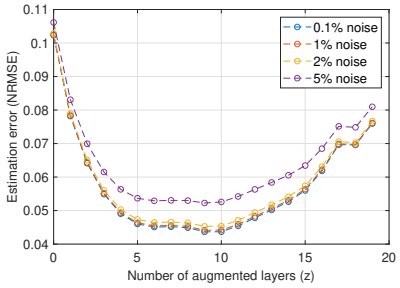

(a) S5,observed

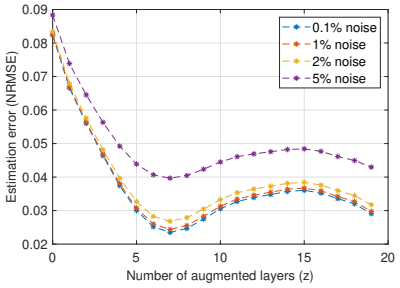

(b) S5,unobserved

Figure 5: Effect of noise levels on response reconstruction.

Finally, it is important to highlight that with the modal-domain adaptation of the proposed delay embedding approach for state observability enhancement, the estimable system dimensionality has been significantly reduced from 116 (2×58) to just 6 (2×3). This substantial reduction in dimensionality has led to a marked decrease in computational requirements. Moreover, this dimensionality remains independent of the physical size of the structure, as only the modes that strongly contribute to the system's dynamics need to be considered. This selective approach further alleviates computational burden while preserving essential system characteristics and not losing on monitoring resolution.

By parameterizing modal information with location-based structural health indices, the proposed methodology remains capable of estimating any linear time-varying (LTV) system without compromising detection precision. Although this aspect has not been particularly emphasized in the current study—given the simplicity of the adopted structure and the availability of system matrices—it holds significant promise for applications requiring high-resolution monitoring of LTV systems, even in scenarios with sparse measurement data.

3.4. Comments on computational benefits

The computations were performed using MATLAB R2022b on a 12th Gen Intel Core i5-12400 processor. When all 58 modes were included in the state model and all 58 *DOFs* (sensors) were instrumented, the computational time was 35.12 seconds. With the same state model size but only the vertical *DOFs* (9 sensors) instrumented, the computation time reduced to 6.52 seconds. When the state model was reduced to the three dominant modes, the time decreased significantly to 0.27 seconds. Introducing lay-

ering (e.g., 6 layers) increased the computation time to 1.12 seconds, which remains computationally efficient. These results highlight that adopting an optimal configuration with fewer sensors, in conjunction with a reduced-order state model that retains essential modal information, leads to significantly faster computations. Additionally, while layering introduces a moderate increase in computation time, it remains well within practical limits, making it a viable approach for real-time applications.

4. CONCLUSION

This study demonstrates the effectiveness of delayed measurement augmentation in modal domain in enhancing the observability of structural systems, particularly under sparse instrumentation. By incorporating time-lagged measurements, the proposed approach significantly improves state estimation accuracy while reducing computational complexity. The modal-domain adaptation further streamlines the process by limiting the estimation to dominant modes, ensuring efficiency without sacrificing precision. Experimental analyses confirm that increasing the number of augmented layers enhances estimation accuracy up to an optimal threshold, beyond which further augmentation provides diminishing returns. Additionally, the approach proves beneficial in mitigating noise effects, making it particularly advantageous in low signal-to-noise ratio conditions. The findings suggest strong potential for extending this method to parameter estimation and structural health monitoring applications, even in complex, time-variant systems. Future work will focus on refining the framework for nonlinear LTV structures, enabling broader applicability in real-world monitoring scenarios.

Funding: This research was partially funded by the Aeronautics Research and Development Board, New Delhi, India, through grant file no. ARDB/01/1052042/M/I and by European project Brighter. BRIGHTER has received funding from the Chips Joint Undertaking (JU) under grant agreement No 101096985. The JU receives support from the European Union's Horizon Europe research and innovation program and France, Belgium, Portugal, Spain, Turkey.

REFERENCES

[1] Gao Fan, Jun Li, and Hong Hao. Dynamic response reconstruction for structural health monitoring using densely connected convolutional networks. *Structural Health Monitoring*, 20(4):1373–1391, 2021.

[2] Jianwei Zhang, Minshui Huang, Neng Wan, Zhihang Deng, Zhongao He, and Jin Luo. Missing measurement data recovery methods in structural health monitoring: The state, challenges and case study. *Measurement*, page 114528, 2024.

[3] SS Law, Jun Li, and Y Ding. Structural response reconstruction with transmissibility concept in frequency domain. *Mechanical Systems and Signal Processing*, 25(3):952–968, 2011.

[4] J LI and SS LAW. Substructural response reconstruction in wavelet domain. *Journal of applied mechanics*, 78(4), 2011.

[5] O. A. Shereena, Subhamoy Sen, and Laurent Mevel. Mitigating ill-posedness in parameter estimation under sparse measurement for linear time-varying systems employing virtual sensor responses. In *Proceedings of the 11th European Workshop on Structural Health Monitoring (EWSHM 2024)*, pages 1–11, Potsdam, Germany, June 2024. NDT.net. doi: 10.58286/29673. URL `https://inria.hal.science/hal-04651217`.

[6] Subhamoy Sen, Antoine Crinière, Laurent Mevel, Frédéric Cérou, and Jean Dumoulin. Seismic-induced damage detection through parallel force and parameter estimation using an improved interacting particle-kalman filter. *Mechanical Systems and Signal Processing*, 110:231–247, 2018.

[7] Cosma Rohilla Shalizi. Methods and techniques of complex systems science: An overview. *Complex systems science in biomedicine*, pages 33–114, 2006.